Incentives for the Use of Depleted Uranium Alloys as Transport Cask Containment Structure*

P. McConnell[+], *R. Salzbrenner, G.W. Wellman, and K.B. Sorenson*

[+]GRAM, Inc., Albuquerque New Mexico 87112 USA
Sandia National Laboratories, Albuquerque New Mexico 87185 USA

INTRODUCTION

Radioactive material transport casks use either lead or depleted uranium (DU) as gamma-ray shielding material. Stainless steel is conventionally used for structural containment. If a DU alloy had sufficient properties to guarantee resistance to failure during both normal use and accident conditions to serve the dual-role of shielding and containment, the use of other structural materials (i.e., stainless steel) could be reduced. (It is recognized that lead can play no structural role.) Significant reductions in cask weight and dimensions could then be achieved perhaps allowing an increase in payload. The mechanical response of depleted uranium has previously not been included in calculations intended to show that DU-shielded transport casks will maintain their containment function during all conditions. This paper describes a two-part study of depleted uranium alloys: First, the mechanical behavior of DU alloys was determined in order to extend the limited set of mechanical properties reported in the literature (Eckelmeyer, 1991). The mechanical properties measured include the tensile behavior the impact energy. Fracture toughness testing was also performed to determine the sensitivity of DU alloys to brittle fracture. Fracture toughness is the inherent material property which quantifies the fracture resistance of a material. Tensile strength and ductility are significant in terms of other failure modes, however, as will be discussed. These mechanical properties were then input into finite element calculations of cask response to loading conditions to quantify the potential for claiming structural credit for DU. (The term "structural credit" describes whether a material has adequate properties to allow it to assume a positive role in withstanding structural loadings.)

DEPLETED URANIUM ALLOYS STUDIED

Because some DU alloys have limited ductility, it has been presumed that no DU alloy can be relied upon to provide a cask containment function (unalloyed DU is typically used for shielding). Mechanical properties were measured for a select group of DU alloys. The chemistry and processing history of these alloys were selected and controlled to produce a broad range of properties and microstructures. The materials matrix was chosen to include effects from intentional alloying additions (e.g., Mo, Nb) which increase the strength, unwanted trace elements (e.g., C, H) which are known to affect the tensile ductility, and heat treatments designed to alter the microstructure.

Table 1 summarizes the DU alloys which were produced for this program. All with the exception of Heat I were cast by Cameco Corporation using a conventional vacuum induction melting process. Heat I was produced by the Y-12 Plant, Martin Marietta Energy Systems, Inc. All of the as-cast materials underwent further processing at the Y-12 Plant which included heat treating to reduce the hydrogen content and/or to control crystal structure and

*Work supported by the United States Department of Energy under Contract DE-AC04-76DP00789.

Table 1. Depleted uranium alloys investigated.

Heat	Nominal Description	Meas. H (ppm)	Meas. C (ppm)
A	unalloyed casting with 200 ppm C	1.53	210
B	unalloyed casting with 200 ppm C +H outgas treatment @630°C/65 hr	0.44	210
C	unalloyed casting with 200 ppm C +H outgas treatment @720°C/35 hr +β cycle (2 times) for grain reduction	0.13	210
D	unalloyed casting with 200 ppm C (thicker casting than Heat A)	1.91	160
E	unalloyed plate with 200 ppm C +H outgas treatment @ 800°C/96 hr, followed by warm rolling at 300°C	0.10	---
F	unalloyed casting with 50 ppm C +H outgas treatment @ 720°C/35 hr	0.07	10
G	3% Mo alloy casting with 50 ppm C +H outgas treatment @ 800°C/24 hr	0.05	53
H	3% Mo alloy casting with 200 ppm C +H outgas treatment @ 800°C/24 hr	0.08	190
I	1.7% Nb alloy casting with 50 ppm C +H outgas treatment @ 800°C/24 hr	0.05	---

rolling to produce plate. The DU alloys were selected to quantify the effectiveness of the hydrogen outgassing treatment in improving ductility and toughness. In addition, the effect of increased additions of molybdenum and reduced levels of niobium, beyond the levels reported in the literature, was also to be characterized.

Metallographic characterization revealed an extremely large grain size (> 1 - 2 mm) in unalloyed DU Heats A, B, D, and F. This large grain size was found in alloys with very low impurity contents which were specially heat treated to remove hydrogen. The grain size of the other unalloyed DU heats (Heats C and E) was reduced to below 0.5 mm. The alloyed DU (Heats G, H, and I) possessed a fine grain size (< 0.1 mm).

MECHANICAL TEST RESULTS

Elastic moduli, tensile strength and ductility, and fracture toughness were measured in this study. The elastic moduli were determined by measuring the density and the ultrasonic velocities of longitudinal and shear waves and calculating the Young's and shear elastic constants. The tensile properties were measured on standard round

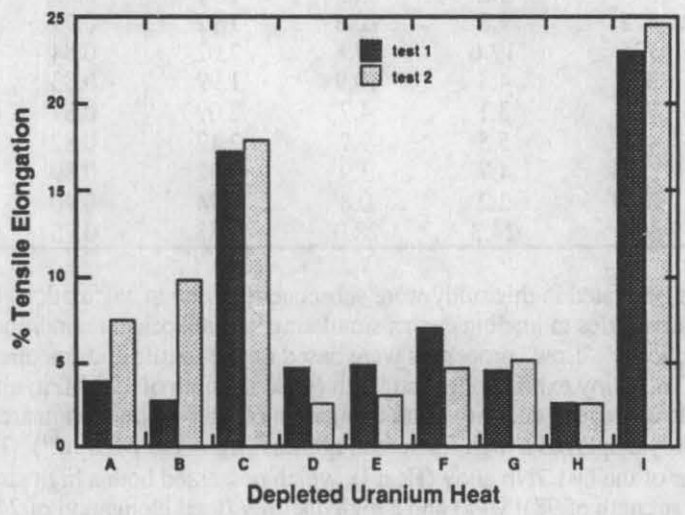

Figure 1. DU alloy tensile ductility test-to-test variation.

tensile specimens. The quasi-static-rate fracture toughness was measured by employing a single-specimen J-integral method, per ASTM E-813, on compact specimens with a net thickness of 22.9 mm. The fracture toughness of the majority of the alloys in this study were elastic-plastic values, J_{Ic}. Equivalent K_{Jc} values were estimated from the J_{Ic} values.

The room temperature mechanical properties for the DU alloys tested are shown in Table 2. Figure 1 is a plot of the tensile ductility measured in separate tests of the same alloy. There is substantial test-to-test variation for Heats A, B, D, E, and F. A sizable amount of test-to-test variation in replicate fracture toughness tests was exhibited for these same heats. The unalloyed Heats A, B, D, and F exhibited very large grain size. The large grain size apparently caused a significant amount of test-to-test variation in duplicate tensile and fracture toughness tests. The average grain size was a large fraction of the cross section of these test specimens, and thus the orientation of single grains could dominate in any particular test result.

The test results show that the fracture toughness of DU can be quite high even though the alloy may exhibit low ductility and/or low impact values. Most of the alloys examined retain elastic-plastic fracture behavior even at -40°C. Such elastic-plastic behavior indicates that failure will not likely occur via brittle fracture when applied stresses are below yield level.

Efforts to reduce impurities (C, H) also resulted in alloys with very large grain sizes (and collateral low ductility). The large grain size caused large variations of the mechanical property measurements within a heat, and thus the direct effect of different levels of C and H could not be accurately determined. Attention to alloy composition and casting process will allow adequately fine grain size to be maintained, along with a suitably high tensile ductility. This can no doubt be accomplished without introducing high levels of interstitial C and H.

The strength properties of DU alloys generally meet or exceed that of 304 stainless steel which is commonly used as the structural material in transport casks. Attempts to increase the strength through alloying often result in a considerable decrease in ductility and fracture toughness. When considered for cask structural applications, DU may be limited more by considerations of ductility and fracture toughness than by strength (i.e., even unalloyed DU may have adequate strength).

Table 2. Average room temperature quasi-static mechanical properties for the depleted uranium alloys.

DU Heat	yield strength (MPa)	ultimate tensile strength (MPa)	total elongation (%)	reduction in area (%)	Young's modulus (10^5 MPa)	shear modulus (10^5 MPa)	fracture toughness K_{Ic} or K_{Jc} MPa-$\sqrt{m}$	impact strength (J)
A	206	374	3.2	6.6	1.94	0.83	107	19
B	206	472	9.8	10.5	1.92	0.79	110	18
C	284	735	17.6	17.8	2.02	0.84	122	18
D	164	374	4.8	10.9	1.99	0.83	103	15
E	382	708	3.1	4.7	2.09	0.87	177	30
F	199	425	5.5	9.7	2.12	0.82	171	37
G	747	1174	4.7	3.9	1.92	0.89	51	4
H	647	1047	2.2	0.8	1.94	0.90	32	1
I	475	981	24.3	28.0	1.83	0.75	151	23

The mechanical properties generated in this study were subsequently used in calculations to determine the response of generic cask geometries to loading events simulating severe accident conditions. Two levels of DU materials properties were chosen. "Low" properties were based on the tensile and fracture toughness test results of unalloyed DU Heat F. This alloy exhibited low strength (yield strength of 199 MPa; ultimate tensile strength of 425 MPa) and low-to-moderate tensile ductility (total elongation of 5.5%; reduction in area of 9.7%). In spite of the limited ductility this alloy displayed a high fracture toughness (K_{Jc} = 171 MPa-$m^{1/2}$). The "high" DU properties were based on the behavior of the U-1.7Nb alloy (Heat I), which possessed both a high strength (yield strength of 475 MPa; ultimate tensile strength of 981 MPa) and a high ductility (total elongation of 24%; reduction in area of 28%). The measured fracture toughness for this material was also high (K_{Jc} = 151 MPa-$m^{1/2}$). The "low"

properties levels were chosen to underestimate the mechanical properties that should be readily available from unalloyed DU with no special processing controls. Representative stress-strain curves were used to provide the constants for the power-law model of the elastic-plastic materials model used in the finite element calculations.

FINITE ELEMENT ANALYSES

Calculations of the response to loading events simulating severe accident conditions were performed for two generic cask geometries, Figure 2. The "Case l" geometry has a stainless steel thickness which was chosen to match that used in an actual cask (i.e., the General Atomics GA-4/9 cask, funded by the U.S. DOE Office of Civilian Radioactive Waste Management). In this cask the stainless steel serves as the primary structural support. Results were compared to those for a second geometry (Case 2) in which the stainless steel thickness was reduced, and the DU assumed the dominant structural role. For Case 1, the thick layer of stainless steel surrounding the DU was chosen by the cask designers to withstand the mechanical loadings from normal use and hypothetical accident conditions. The DU layer was sized to provide the requisite shielding (accounting for the stainless steel shielding). In Case 2, the thick stainless steel layer was reduced to a thin sheet; the thickness of the DU was appropriately increased over that used in Case 1 to provide for a constant amount of shielding between the two cases. The structural responsibilities of the DU increased in Case 2, since only thin stainless steel layers were present on either side of the DU.

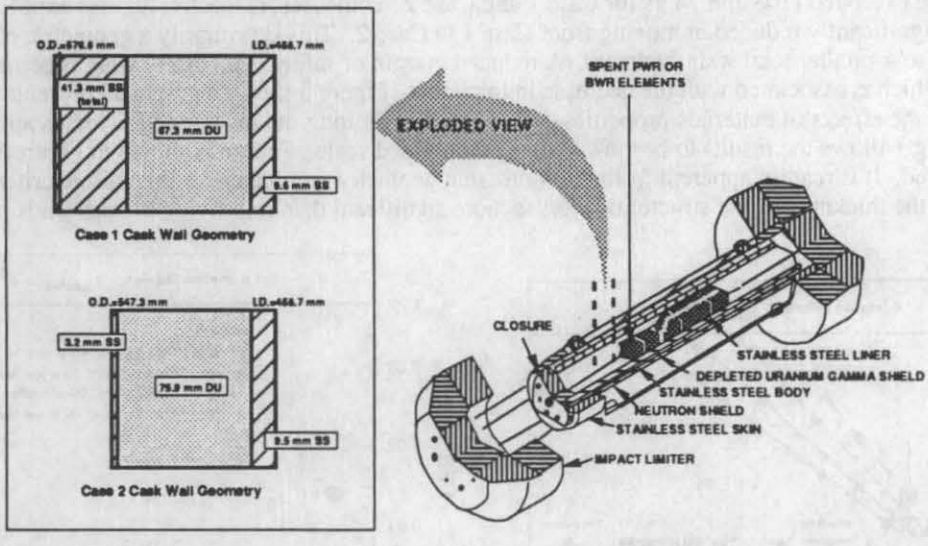

Figure 2. Schematics of the two cask designs for structural analyses.

The mechanical response of the DU layer was assessed in terms of three different failure criteria to determine whether DU assumed the increased structural responsibility required by changing the cask design from Case 1 to Case 2.

First, the maximum tensile stress in the DU layer was calculated as a function of applied acceleration ("g^s") and then compared with U.S. Nuclear Regulatory Commission Regulatory Guide 7.6 stress allowable values. The NRC design guidance for transport casks (U.S. NRC 1978) imply that the cask should be able to elastically withstand all loads applied during normal use or hypothetical accident conditions. Specifically, it is generally assumed that application of such loads will not cause through-wall plasticity. If this condition is applied, the necessity of having a material capable of undergoing extreme plastic deformations is greatly diminished. Theoretically, only a limited tensile ductility might be required to withstand local plastic deformation (particularly when the fracture toughness is high). As a practical matter however, it is prudent to require sufficiently high ductility as a means of demonstrating a margin of safety against tearing failure. DU alloys which exhibit moderate tensile ductility (e.g., elongations >10%) may provide sufficient margin. In the analyses, the cask was treated as a simply supported beam subjected to multiple gravity loading. Elastic response of the cask materials was assumed. For the simulated side drop events, stresses were predominantly primary membrane. For such a loading condition, the Regulatory Guide allows a stress which is smaller than the lesser of 2.4 S_m or 0.7 S_u. The value of S_m is based on the ASME Design Stress Intensity, and is, for ferritic steels, the smaller of two-thirds of

the yield strength, S_y or one-fourth of the ultimate strength, S_u, of the alloy. DU is not listed as an ASME Code material, but for the purposes of this feasibility study was treated with the same restrictive rules as those which govern ferritic steels since DU alloys can, under certain conditions, fail in a brittle manner. For both the low and high property DU alloys, the allowed S_m is thus one-fourth S_u. The allowable stress (=2.4 S_m = 0.6 S_u) is therefore 255 MPa for the "low" property DU, and 589 MPa for the "high" property DU alloy. For comparison purposes, the ASME Design Stress Intensity for 304 stainless steel (S_y = 207 MPa) is 138 MPa and the maximum allowable stress is 331 MPa. The first stress-based failure criterion occurs therefore when:

$$2.4\ S_m / S_a < 1 \qquad \text{Equation 1}$$

where S_a is the maximum applied tensile stress.

Table 3 lists the factor of safety in terms of stress in the DU layer when the casks from Case 1 and Case 2 are subjected to an applied lateral g-load. The factor of safety, FS, is the ratio of the stress allowable to the maximum calculated stress in the DU layer (Eq. 1). When the FS ratio is less than unity, the DU fails this stress-based design criterion. Even the "low" property DU for both cask designs maintains its structural integrity at acceleration levels greater than the 50 g level expected for the nine-meter drop with impact limiters (Osborne et al. 1989). The "high" property DU alloy can withstand high levels of acceleration before the regulatory stress allowables are exceeded (103 and 74 gs for Case 1 and Case 2 geometries, respectively). As expected, the margin to failure is significantly reduced in moving from Case 1 to Case 2. This is primarily a geometric effect in moving from a larger to a smaller total wall thickness. A reduced margin of safety is precisely what is being traded for the lower mass which is associated with the decrease in thickness. Figure 3 shows a graphical presentation which demonstrates the effects of materials properties and geometry. Plotting the inverse of FS versus applied acceleration (g's) allows the results to be viewed on a compressed scale. Failure is shown in Figure 3 if a value of one is exceeded. It is readily apparent from the figure that geometry dominates for this failure criterion: the effect of increasing the thickness of the structural layers is more significant than improving the materials properties.

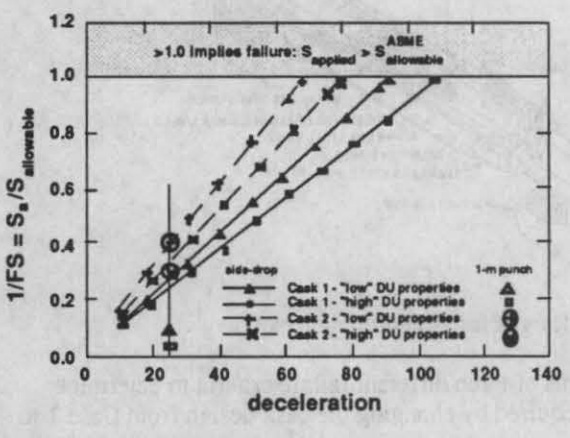

Figure 3. The inverse of the Factor of Safety for the ASME Design Stress Intensity failure criterion as a function of applied acceleration. (Case 1 is thick stainless steel layer, Case 2 is thin stainless steel.)

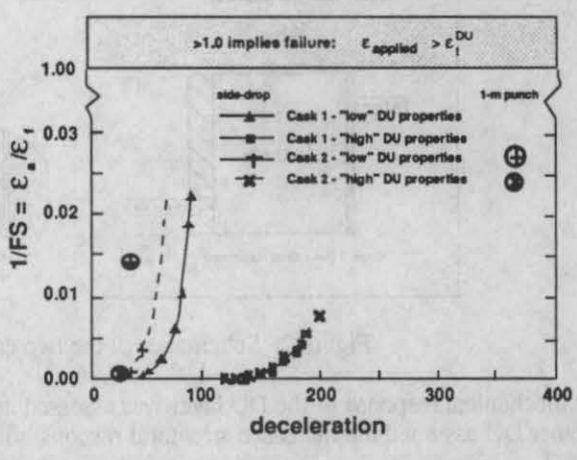

Figure 4. The inverse of the Factor of Safety for the True Strain-to-Failure failure criterion as a function of applied acceleration. (Case 1 is thick stainless steel layer, Case 2 is thin stainless steel.)

A second failure criterion is based on the strain-to-failure. This deformation failure criterion presents a more rational basis for determining the actual physical response of a structure than the NRC/ASME stress-based method described above. In applying this method, a finite element calculation of the strain in the DU layer was performed for the two geometries and the two levels of DU properties. The cask ends were constrained and a gravity load was applied. Nonlinear materials properties were used. The applied acceleration was increased until through-wall yielding of the cask was computed. A power-law constitutive model (JAC3D, a nonlinear, quasi-static, finite element computer program) was used for these calculations. This type of analysis is incapable of determining the

Table 3. The Factors of Safety (FS) calculated for the two cask designs using the ASME Design Stress Intensity and the True Strain-to-Failure Criteria.

	FS_σ* for ASME Design Stress Intensity				FS_ε** for True Strain Failure Criterion			
	Case 1		Case 2		Case 1		Case 2	
applied acceler.	"low" props.	"high" props.	"low" props.	"high" props.	"low" props.	"high" props.	"low" props.	"high" props.
(g^s)								
10	9.4	10.4	6.7	7.4				
20	4.7	5.2	3.4	3.7				
30	3.1	3.5	2.2	2.5				
40	2.3	2.6	1.7	1.9			728	
50	1.9	2.1	1.3	1.5	31865		303	
60	1.6	1.7	1.1	1.2	1133			
70	1.3	1.5	0.9	1.1	418			
80	1.2	1.3		0.9	160			
90	1.0	1.2			53			
100	0.9	1.0						
110		0.9						
120								115438
130								9850
140						10579		2419
150						2253		1123
160						991		639
170						438		349
180						276		272
190						226		180
200								132

*FS_σ= ASME $S_{allowable}/S_a$ **$FS_\varepsilon = \varepsilon_f/\varepsilon_a$

dynamic effects of an actual side drop and also ignores the behavior of impact limiters. Nonetheless, this analysis is very effective in providing the data required to assess the structural response of DU.

For every applied "g" the maximum true strain in the DU layer was calculated and compared to the true strain to failure determined from tensile test results. The failure criterion for this calculation is thus the true tensile strain to failure, ε_f, divided by the finite element calculation of the true applied plastic strain in the DU, ε_a.

$$\varepsilon_f / \varepsilon_a < 1 \qquad \text{Equation 2}$$

The strain-based FS at various applied g^s are also presented in Table 3. Figure 4 is a graphical presentation of the data in which the inverse of FS is plotted as a function of applied acceleration. From the figure, it is apparent that the DU is far from failure as defined by the true strain to tensile failure. The calculations were terminated when through-wall yielding was found in the DU. This presents a high level of conservatism and provides agreement with the implied design requirements for a fully elastic response. In contrast to the results of the ASME method where the thickness of the various layers dominated the calculation of the FS, it is the materials properties which dominate the determination of the FS which is based on the strain-to-failure. Using a strain-based failure criterion provides the opportunity to judge the response of structures using a more fundamental understanding of actual materials behavior.

A third fracture mechanics failure analysis must be considered when using a material such as DU which can fail in a brittle manner under certain severe conditions. Fracture mechanics analyses are based on comparing the driving force for brittle fracture to the material's inherent resistance to fracture, a property known as fracture toughness. For brittle fracture the fracture toughness is measured in terms of the linear-elastic value designated as K_{Ic}. The fracture toughness of the majority of the alloys measured in this study were determined as ductile elastic-plastic values, J_{Ic}. Equivalent K_{Jc} values were estimated from the J_{Ic} values.

The linear elastic stress intensity in the region of a flaw provides a driving force for crack extension, and can be calculated from the following relationship:

$$K_I = S_a C (\pi a)^{1/2} \qquad \text{Equation 3}$$

where K_I is the applied stress intensity, C is a geometry factor ($\cong$1.2), and "a" is the flaw depth. When the K_I exceeds the fracture toughness (i.e., K_{Ic} or K_{Jc}), crack growth is predicted.

As a means of determining the sensitivity of the DU to brittle fracture for the casks in this study, Equation 3 can be rearranged as to calculate the critical flaw size for brittle fracture, a_c:

$$a_c = (1/\pi) [(K_{Jc})/(S_a * C)]^2 \qquad \text{Equation 4}$$

with K_{Jc} substituted for K_I. Thus the largest flaw that can be tolerated by the structure at a specific applied stress level can be computed. The overall cask system (which would include impact limiters) would be designed to prevent applied through-wall stresses which are above the yield strength level of each of the materials used. Equation 4 is only valid in the elastic regime, and thus the yield strength will be used for the calculation of the largest flaw size that can be tolerated. The "high" property DU has a lower fracture toughness (i.e., 151 MPa-$m^{1/2}$) than the "low" property DU and thus this value is used as an example. The "high" yield strength is 475 MPa. Substituting these values into Equation 4 produces a value for the critical flaw size, a_c, equal to 25.7 mm. Non-destructive evaluation (NDE) techniques are available which can locate all flaws which are even a small fraction of this value. The above calculation with improbable yield-level applied stress demonstrates flaw tolerance of DU. Proper design of the cask with impact limiters would reduce the applied stress significantly, and thus the allowed (i.e., non-critical) flaw size would be even greater. Potential for brittle fracture can be eliminated by: i) NDE inspection to assure that all flaws which are present are significantly smaller than $\cong$25 mm in depth, and/or ii) designing to guarantee that applied stress will always be below an appropriate value. Such requirements would result in a high level of conservatism against brittle fracture.

Further finite element analyses of the four cask geometry/materials combinations were conducted to model a one-meter side drop onto a 152 mm diameter puncture pin. The puncture event was analyzed as a non-linear dynamic impact event. The power-law hardening constitutive model in PRONTO 3D was used for these computations. Additional mass was assigned to the cask ends to represent the impact limiters which were not specifically modeled. The pin contacted the cask at mid-span on the transverse center line. This location causes the maximum stress in the cask wall. In applying the stress-based and strain-based failure criteria described above, the resulting stress and strain combinations from these calculations were so low that failure from a drop onto a pin does not present a credible failure potential for any of these geometry and material combinations. The values are plotted on Figures 3 and 4 at a nominal value of 25 g and indicate the large factor of safety inherent to the DU for the one-meter punch condition.

DISCUSSION

Results from the analyses described above indicate that certain DU alloys have sufficient strength, ductility, and toughness to be considered for structural applications in transport casks, particularly true when cask design response to various accident conditions precludes through-wall yielding. The data are not extensive enough however, to act as the basis for qualifying a particular material in this regard. For the structural analysis calculations shown, the room temperature properties were used as the basis of the materials model. If similar calculations are to be performed to support a claim for structural credit of DU in a specific design, the applicable mechanical properties must be determined at rates and temperatures which match those of the worst loading conditions. Further, the finite element calculations should be conducted for the specific cask design which includes all relevant features, including: cask bottom end, cask closure end, impact limiters, etc.

The most obvious benefit of qualifying DU as a structural component in transport casks results from a reduction of the thickness of the overall structure, while maintaining the necessary structural integrity. This allows a reduced cask body mass and an increased spent-fuel payload potential. In those casks which use a particularly expensive material (e.g., stainless steel or titanium) the ability to partially or completely eliminate such material may lead to an important reduction in the cost of fabrication through lower cost for raw materials. In addition, there is a cost reduction associated with the increased ease of fabricating (forming, welding, inspecting, etc.) and assembling

thinner sections. For cask designs which approach dimensional and/or mass limitations, the qualification of DU as a positive contributor to the structural integrity (thereby reducing the requirement for other materials) may provide a significant advantage. Potential mass reduction in the cask without sacrificing payload may provide the necessary margin if the gross cask mass becomes a certification issue. For the current example (i.e., Case 1 vs. Case 2), the mass savings from the reduction in the thickness of the stainless steel amounts to ≅1550 kg. This is ≅10% of the overall cask mass (or ≅ 6.3% for the fully loaded cask with impact limiters), and may be of significance for an actual cask which is near the maximum allowable mass, with scant margin for contingencies such as tie-downs, skids, or support cradles.

In any event, the use of DU in cask design may be more prudent than the use of lead for shielding due to such factors as lead melting or lead slump (Ammerman, 1992) which may affect the integrity of the stainless steel containment.

The DU in both cask geometries is surrounded by two layers of stainless steel. Stainless steel offers corrosion resistance and decontamination advantages, and even when present in only thin sections (i.e., Case 2) has an important effect on the structural response. The highly ductile and tear-resistant stainless steel provides additional conservatism against brittle fracture by spreading any locally applied stresses thus acting as a barrier to brittle fracture propagation.

Heat transfer characteristics would be enhanced if the thickness of the stainless steel could be reduced. A further heat transfer benefit would be gained if one or more interfaces could be eliminated by removing a stainless steel layer in designs in which DU can assume structural responsibility.

Problems which must be addressed to pursue structural credit for DU in cask design are not insignificant, however. Foremost may be the inherent regulatory reluctance to the use of any material for cask containment which may fail in a brittle manner, no matter how remote that possibility. Second are the procedural issues related to ASME Code acceptance of DU for structural applications and the standardization of candidate DU alloys through ASTM. Finally, there are the fabrication issues related to construction of a cylindrical body of DU for containment. DU shields are constructed of semi-circular rings which, for structural application, may require welding or linkage by means of axial tie-rods. Concerns over the properties of the welded regions or the bending strength of the segmented DU layer require analysis.

CONCLUSIONS

Materials properties of a broad range of DU alloys have been measured. These mechanical properties form the basis for finite element calculations that suggest that certain DU alloys can be assigned a structural role in specific transport cask designs. The effect of gaining structural credit for the DU allows the use of stainless steel to be reduced. In this example, a thick layer of stainless steel was eliminated, which resulted in a direct mass reduction of > 6% for the fully loaded cask. This is considered highly significant due to potential weight problems in cask design and in the potential for increase in payload.

REFERENCES

Ammerman, D. J., Wellman, G. W., and Heinstein, M. W., *Comparison of Elastic and Inelastic Analyses*, Proceedings of PATRAM '92, The 10th International Symposium on the Packaging and Transportation of Radioactive Materials, September 13-18, Yokahama, Japan (1992).

Eckelmeyer, K.H., *Uranium and Uranium Alloys*, in Metals Handbook, Volume 2, 10th Edition, ASM International, Materials Park, OH, USA (1991).

Osborne, D., Koploy, M., and Pickering, L., *Analysis of the Non-Cylindrical GA-4 and GA-9 Spent Fuel Casks*, Proceedings of PATRAM '89, The 9th International Symposium on the Packaging and Transportation of Radioactive Materials, June 11-16, Oak Ridge National Laboratory, Washington, DC, USA (1989).

Regulatory Guide 7.6: Design Criteria for the Structural Analysis of Shipping Cask Containment Vessels, U.S. Nuclear Regulatory Commission, Revision 1 (1978).